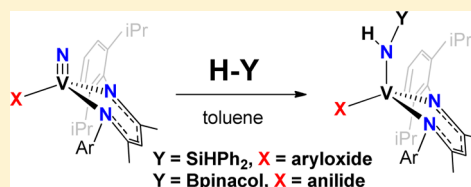# Addition of Si−H and B−H Bonds and Redox Reactivity Involving Low-Coordinate Nitrido−Vanadium Complexes

Rick Thompson,[‡] Ba L. Tran, Soumya Ghosh, Chun-Hsing Chen, Maren Pink, Xinfeng Gao, Patrick J. Carroll,[‡] Mu-Hyun Baik, and Daniel J. Mindiola*[,‡]

Department of Chemistry and Molecular Structure Center, Indiana University, Bloomington, Indiana 47405, United States
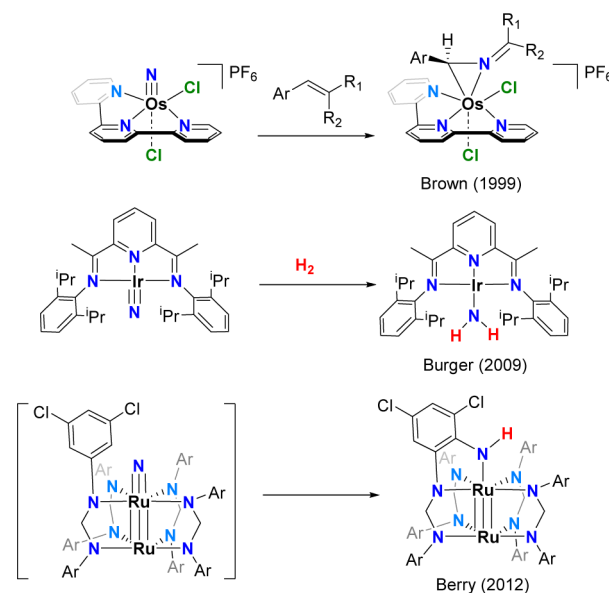
S *Supporting Information*

ABSTRACT: In this study we enumerate the reactivity for two molecular vanadium nitrido complexes of [(nacnac)V≡N(X)] formulation [nacnac = (Ar)NC(Me)CHC(Me)(Ar)⁻, Ar = 2,6-(CHMe₂)₂C₆H₃); X⁻ = OAr (**1**) and N(4-Me-C₆H₄)₂ (Ntolyl₂) (**2**)]. Density functional theory calculations and reactivity studies indicate the nitride motif to have nucleophilic character, but where the nitrogen atom can serve as a conduit for electron transfer, thus allowing the reduction of the vanadium(V) metal ion with concurrent oxidation of the incoming substrate. Silane, H₂SiPh₂, readily converts the nitride ligand in **1** into a primary silyl−amide functionality with concomitant two-electron reduction at the vanadium center to form the complex [(nacnac)V{N(H)SiHPh₂}(OAr)] (**3**). Likewise, addition of the B−H bond in pinacolborane to the nitride moiety in **2** results in formation of the boryl−amide complex [(nacnac)V{N(H)B(pinacol)}(Ntolyl₂)] (**4**). In addition to spectroscopic data, complexes **3** and **4** were also elucidated structurally by single-crystal X-ray diffraction analysis. One-electron reduction of **1** with 0.5% Na/Hg on a preparative scale allowed for the isolation and structural determination of an asymmetric bimolecular nitride radical anion complex having formula [Na]₂[(nacnac)V(N)(OAr)]₂ (**5**), in addition to room-temperature solution X-band electron paramagnetic resonance spectroscopic studies.

INTRODUCTION

The long-standing interest in metal nitrides stems from their relevance in metal-mediated conversion of dinitrogen into ammonia. Over the years, metal−nitride chemistry has developed into an interesting research area solely based on the unusual bond activation and redox activity that these molecules often exhibit. The terminal nitride (N³⁻) ligand can behave either nucleophilically or electrophilically depending on a number of factors including the metal (or ligand) character of the lowest unoccupied molecular orbital (LUMO), ligand field strength, and number of d electrons at the metal center.[1,2] Moreover, complexes featuring an electrophilic nitride functionality undergo rich multielectron reactions[3−5] and are generally confined to mid- to late-transition metals in high oxidation states, which are unstable due to the population of π*-antibonding orbitals.[6] Accordingly, substrates react at the terminal nitrogen atom with concomitant two- or three-electron reduction at the metal center. For example, oxidative chemistry at the nitride ligand to form a nitrosyl ligand,[3,7] and reductive hydrogenation to generate metal−amide (M−NH₂) ligands,[6] have been demonstrated previously (Scheme 1). Hydrogen atom sources can also convert the nitride group on iron to NH₃.[8] These transformations hold important relevance to the Haber−Bosch nitrogen fixation reaction in which dinitrogen is converted into ammonia.[6] Additionally, electrophilic nitride ligands also mediate intramolecular C−H activation[9−11] and insertion of the nitride functionality into B−C bond and C−C bonds (Scheme 1).[12,13] Lastly, the reductive coupling of two monomeric electrophilic nitrides to

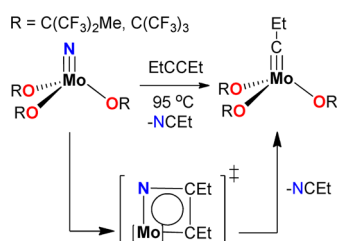**Scheme 1. Some Representative Examples of Reactive Electrophilic Nitrides Featuring Mid- to Late-Transition Metals**

form dinitrogen, which constitutes the microscopic reverse reaction of dinitrogen cleavage, has been demonstrated to proceed via a bimolecular pathway for osmium, iron, ruthenium, and rhodium.[10,14−16]

In contrast, early metal nitrides are generally stable, owing to their preference for high oxidation states. In fact, terminal metal nitrides often constitute pertinent thermodynamic sinks and are encountered during molecular dinitrogen cleavage reactions[17−19] and cross-metathesis involving metal alkylidynes and nitrile substrates.[20] Interestingly, the electronics for the latter reaction can be altered by installing electron-withdrawing ligands, rendering the nitride functionality more reactive than (or comparable to) the corresponding alkylidyne (Scheme 2).[21,22] These systems are therefore poised to be important for

Scheme 2. Conversion of Mo−Nitride to Mo−Alkylidyne Species for Catalytic Alkyne−Nitrile Cross-Metathesis

alkyne−nitrile cross-metathesis catalysis due to the reactive nature of the nitride precatalyst.[23,24] Although the theoretically derived bond dissociation energy (BDE) of ∼165 kcal/mol for the molybdenum−nitride triple bond in a pseudotetrahedral environment is high,[25,26] recent work[27,28] suggests that the nitride functionality is still susceptible to further reactivity. Nevertheless, there still exists the enduring perception that early metal nitrides serve more as spectator ligands rather than being a reactive functionality.

We were therefore prompted to investigate whether vanadium nitride species can be reactive due to the inherent accessibility of a multitude of common oxidation states from V(II) to V(V). Cummins has demonstrated that a vanadium nitride anion can undergo complete N atom transfer to CO,[29] and we have shown that a neutral nitride ligand can engage in incomplete transfer to CO, CNR,[30] and S.[31] The lack of detailed reactivity studies of early 3d metal nitrides, namely, from groups 3−5, prompted our endeavor toward a readily accessible synthesis of well-defined molecular vanadium nitrides for systematic studies involving redox chemistry at the vanadium center but also involving transformations at the nitride functionality.

We recently communicated the synthesis of (nacnac)V≡N(N[R]tolyl) (R = 4-MeC6H4 (tolyl, **2**); 2,4,6-Me₃C₆H₂ (Mes)) [(nacnac = [ArNC(CH₃)]₂CH⁻, Ar = 2,6-^{i}Pr₂C₆H₃)] and its preliminary reactivity with π-acids by taking advantage of the vanadium(V/III) redox couple.[32] Likewise, this work was expanded to the aryl oxide supported nitride derivative (nacnac)V≡N(OAr) (**1**).[33] Herein, we delineate additional reactivity involving (nacnac)V≡N(Ntolyl₂) and (nacnac)V≡N(OAr) (Ar = 2,6-^{i}Pr₂C₆H₃). Compound **1** reacts with diphenylsilane to convert the nitride ligand to a primary silylamide with concomitant two-electron reduction at vanadium. Similar chemistry is also observed with pinacolborane, resulting in the corresponding borylamide. Lastly, we demonstrate that (nacnac)V≡N(OAr) can be reduced by one
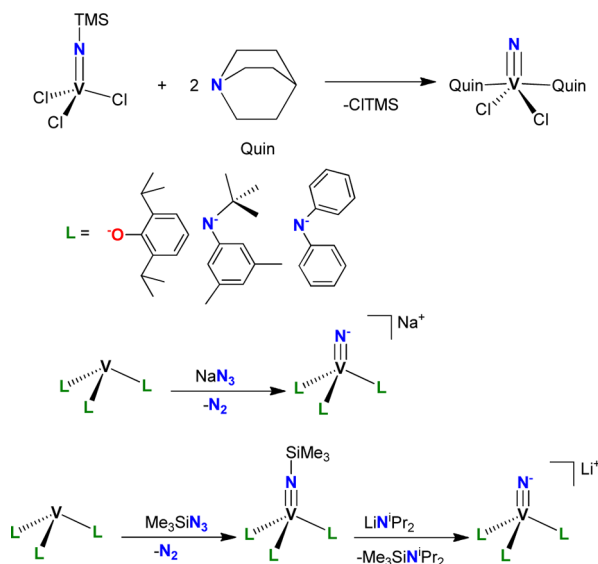
electron to form the nitride radical anion [(nacnac)V≡N(OAr)]⁻•, which exists as an asymmetric dimer in the solid state. All metal complexes reported herein were fully characterized by multinuclear (¹H, ¹³C, ⁵¹V) NMR spectroscopy, room-temperature magnetic susceptibility measurement, Fourier transform infrared (FT-IR) spectroscopy, and single-crystal X-ray diffraction (XRD) whenever possible. The structures of the sodium salt of the radical anion [(nacnac)-V≡N(OAr)]⁻• and its solvated derivative were also examined by X-band electron paramagnetic resonance (EPR) spectroscopy.

■ RESULTS AND DISCUSSIONS

Synthesis of Molecular Vanadium Nitride Complexes. There are two divergent synthetic approaches to isolating molecular vanadium nitrides: (1) Lewis base (L = pyridine, quinuclidine)-promoted halogen abstraction of a trimethysilyl group from metastable Cl₃V≡NSiMe₃ to produce either polymeric chain or monomer nitrides with the formula L₂Cl₂V≡N and Me₃SiCl depending on the base used[34,35] (Scheme 3) and (2) the oxidation of a low-coordinate

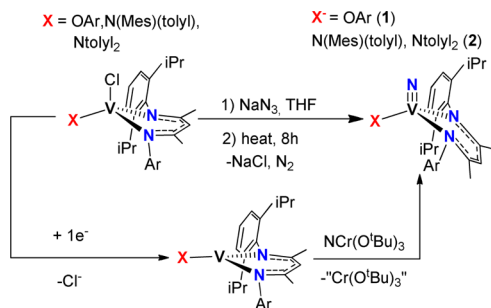**Scheme 3. Reported Syntheses of a Neutral and Anionic Vanadium Nitrides**

vanadium(III) precursor with azide sources Me₃SiN₃ or NaN₃ to engender anionic vanadium(V) nitride with concomitant N₂ extrusion and a two-electron oxidation of V(III).[36−39] Employing Me₃SiN₃ leads to formation of a trimethylsilyl imido vanadium compound and subsequent desilylation with nucleophiles such as lithium diisopropylamide renders the anionic nitride vanadium(V) product.[39,40] Alternatively, NaN₃ provides direct access to anionic nitride vanadium without need of deprotection. The latter synthetic approach is more feasible because the metastable precursor is avoided, and complexes of vanadium(III) are readily accessible.

The pseudotetrahedral geometry is critical to the stability of anionic nitride complexes, which can be rationalized because the trans influence of the nitrido ligand is negligible given that there is no ligand directly trans to the nitride competing for orbital overlap. Additionally, low-coordinate tetrahedral geometry provides the available three metal orbitals to form the

required 1σ and 2π bonds to make the formal metal–nitrogen triple bond. Considering literature precedent, we opted to conserve the pseudotetrahedral geometry at vanadium.

On the basis of the above consideration and rationale, we found two routes for assembling terminally bound and neutral nitride ligands on vanadium. One route is to treat the precursors [(nacnac)VCl(OAr)] and [(nacnac)VCl(Ntolyl$_2$)] with NaN$_3$ to yield [(nacnac)V≡N(OAr)] (**1**) and [(nacnac)-V≡N(Ntolyl$_2$)] (**2**) via metastable azide intermediates (Scheme 4, azide intermediates are not shown for clarity).

Scheme 4. Preparation of Neutral Vanadium(V) Complexes Having the Terminal-Bound Nitride Ligand[a]

[a]Ar represents the aryl group 2,6-^{i}Pr$_2$C$_6$H$_3$.

Complete physical characterization for **1** and **2** has been reported elsewhere (Scheme 1).[32] Compound **1** can be also obtained from complete intermetal N atom transfer with N≡Cr(O^{t}Bu)$_3$[41] by delivering the nitrogen atom to the masked vanadium(II) synthon (nacnac)V(Ntolyl$_2$) in an overall three-electron reaction.[42] We demonstrate here that this similar strategy can also be expanded to the three-coordinate V(II) complex (nacnac)V(OAr) using N≡Cr(O^{t}Bu)$_3$ as an N atom source. Both of these vanadium(II) materials can be readily prepared in multigram quantities by 1e$^-$ reduction of the precursors [(nacnac)VCl(OAr)] and [(nacnac)VCl(Ntolyl$_2$)] (Scheme 4).

Density Functional Theory Studies of the Mononuclear and Neutral Vanadium Nitrides. To elucidate the electronic structure of the vanadium nitride and predict its reactivity, we relied on density functional theory (DFT) calculations. The optimized geometry of **1** agrees well with the experimentally determined solid-state structure established by single-crystal XRD studies. The calculated vanadium–nitride distance is 1.549 Å (actual = 1.565(4) Å), consistent with a triple bond between vanadium and N^{3-} and a Mulliken–Mayer bond order of 2.7. Table 1 provides a complete comparison of the bond angles and distances between the computed and crystallographically characterized structure of (nacnac)V≡N(OAr). Aryloxide and nacnac are reputable π-donors in cases where an electron-deficient metal center is involved; however, in this system, V–O and V–N(nacnac) interactions are essentially σ-based single bonds with Mulliken–Mayer bond orders of ~0.6. The bent angle of V–O–C$_{ipso}$ = 164.05° in the computed nitride complex is slightly more linear than the actual structure, but the molecular orbital analysis revealed no π-donation from the aryloxide. The lack of π-donation from the aryloxide and nacnac ligand into the d^0 vanadium is interesting, despite the availability of two empty metal π-orbitals of matching symmetry capable of accepting π-electrons. Nonetheless, this electronic picture corroborates the crystallographic

Table 1. Comparing the Selected Bond Distances and Angles of the Calculated (DFT) Structure to those of the Measured (XRD) Structure of 1
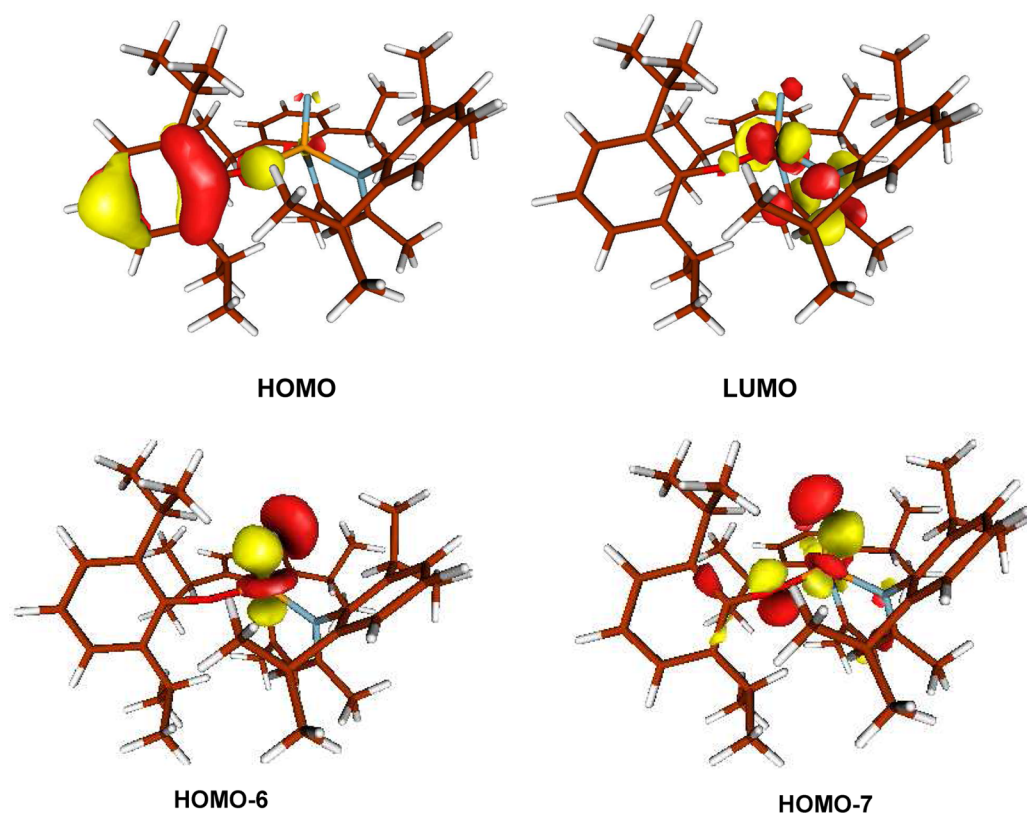
bond distances and angles	XRD[a]	calculated[a]
V1–N1	1.956(2)	1.9726
V1–N2	1.947(4)	2.0085
V1–N3	1.565(4)	1.5493
V1–O1	1.814(3)	1.8175
N3–V1–O1	114.75(18)	113.66
V1–O1–C(ipso)	150.4(3)	164.05
N1–V1–N2	97.85(15)	96.30
N1–V1–N3	110.58(17)	111.31
N1–V1–O1	109.46	110.94
N3–V1–O1	114.76(18)	113.15

[a]Distances are reported in angstroms, and angles are reported in degrees.

evidence that the aryloxide and nacnac ligands are two- and four-electron donors, respectively, suggesting compound **1** contains a relatively electron-deficient vanadium(V) center.

As anticipated for a vanadium(V) complex all five metal d-dominated frontier orbitals are empty. The highest occupied molecular orbital (HOMO) is composed primarily of aryloxide ligand-based orbitals (Figure 1). The lowest unoccupied molecular orbital (LUMO) is primarily composed of a metal-based d-orbital in the xy-plane with additional strong contributions from the π* of the nacnac ligand. Some of the nitride ligand-based bonding orbitals are quite stable and shown as HOMO−6 and HOMO−7 in Figure 2. They are ~1.1 eV lower in energy than the HOMO. The presence of an aryloxide ligand breaks the local symmetry at vanadium to C_s leading to the observed rehybridization of the lone pairs, but more importantly, this feature increases the energy of the d$_{xz}$ orbital via a σ* interaction. Hence, the d$_{xz}$ orbital cannot effectively engage in π-interaction with the lone pair on nitrogen (HOMO−6) (Figure 2). The nature of this rehybridization propels the nitrogen lone pairs in the vanadium system to be higher in energy. The high-energy lone pair is most likely responsible for the observed reactivity of vanadium nitride as a competent nucleophile. For a deeper understanding of the vanadium nitride electronic structure and its governance on the general reactivity relative to an electrophilic nitride, we turned to Mayer's TpOs(N)Cl$_2$ (Tp$^-$ = tris(pyrazolyl)borate)[43] because this system has been examined by DFT calculations and represents a longstanding model as an unusually reactive electrophilic nitride complex. Analogous to our vanadium nitride species, the orbitals hosting the nitrogen lone pair and the Os≡N π-bonding situate roughly −1.0 eV below the HOMO. The chief difference in the electronic structure that distinguishes the osmium nitride from the vanadium nitride is the amount of nitrogen character in the LUMO and LUMO+1 for the osmium system. For vanadium, these orbitals are more localized on the metal and supporting ligands, with minimal contribution from the nitride nitrogen. Therefore, a good description of the nature of the nitride functionality depends on its LUMO and whether it has more ligand or metal orbital contribution. On the basis of this premise, DFT suggests the nitride ligand in **1** (and likely **2**) to be more nucleophilic in character. By matter of opinion, in the instances where redox levels change, it is sometimes considered inappropriate to describe the nitride as either nucleophile or electrophile, but rather should be described as a reductant or oxidant (or in

HOMO

LUMO

HOMO-6

HOMO-7

Figure 1. Above molecular orbitals show two lone pairs on the terminal nitrogen important for understanding the bonding and reactivity of vanadium nitride. HOMO−7 is the highest energy lone pair on the nitrogen, which is 1.1 eV lower than the HOMO.
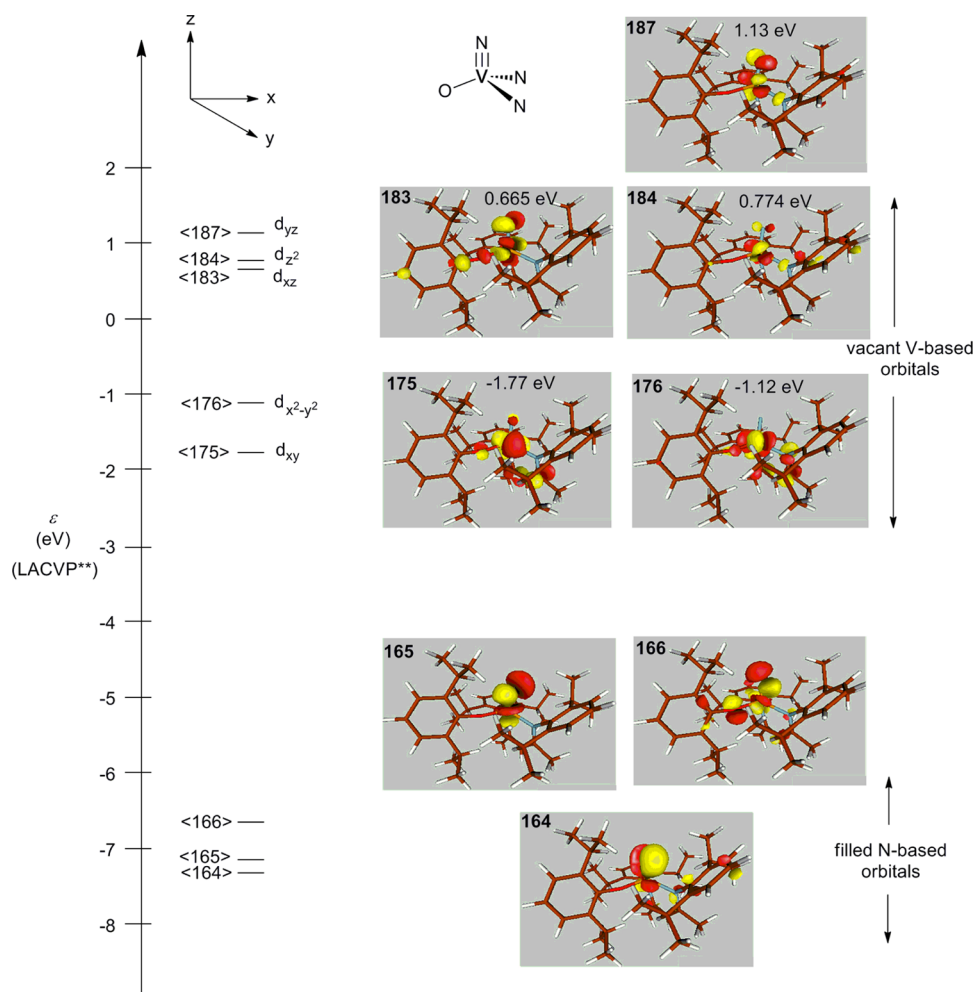
some instances, both). As a result, some readers might find the term nucleophilic or electrophilic inappropriate.

Addition of Si−H and B−H Bonds to the Nitride Functionality. The conversion of mononuclear (PBD)Ir≡N to Ir−NH$_2$ (PBD = 2,6-(2,6-^{i}Pr$_2$C$_6$H$_3$−N=CMe)$_2$C$_5$H$_3$N) was achieved via hydrogenation of the corresponding nitride species with dihydrogen[6,10] and, more recently, via hydrostannylation followed by hydrolysis.[44] Additionally, the transient nitride species N≡Ru$_2$(D(3,5-Cl$_2$)PhF)$_3$, where (D(3,5-Cl$_2$)PhF = N,N′-bis(3,5-dichlorophenyl)formamidinate),[11,45] (^{iPr}PDI)-Co≡N (^{iPr}PDI = 2,6-(ArN=CPh)$_2$C$_5$H$_3$N; ^{i}Pr = 2,6-^{i}Pr$_2$C$_6$H$_3$),[46] and (C$_5$Me$_5$)$_2$U≡N(N(SiMe$_3$)$_2$)[9] have been implicated in the formation of metal−amido via intramolecular C−H activation. In all cases, there is little evidence for legitimate formation of a true M−N triple bond; instead, nitrene-like character is suggested. Instances of open-shell nitride species have also been reported. These late-metal complexes have been found to be unstable toward dimerization, generating a dinitrogen complex in the case of both iridium[47] and rhodium.[48] The use of a slightly different supporting ligand on rhodium led to isolation of a bridging dirhodium nitridyl dimer in which a considerable amount of the singly occupied molecular orbital is composed of nitrogen character as seen by both EPR spectroscopy as well as calculations.[49] The exemplary hydrogenation reaction of a metal−nitride species is of relevance regarding the important conversion of dinitrogen to ammonia as proposed in the Chatt dinitrogen fixation cycle. Therefore, we promptly explored the reactivity of **1** and **2** with dihydrogen. The addition of H$_2$ (1 atm) to a deuterated benzene (benzene-d_6) solution of either of these two nitrides did not lead to a reaction when gauged by ^{1}H NMR spectroscopy. However, substitution of H$_2$ for H$_2$SiPh$_2$ allowed

for reduction of the vanadium nitride functionality to render green [(nacnac)V{N(H)SiHPh$_2$}(OAr)] (**3**) (Scheme 5) in 61% yield from recrystallization of a saturated ethereal solution at −37 °C. To date we have not pursued other silanes in detail apart from HSiEt$_3$ but suspect that the use of bulkier or tertiary silanes may require heating to achieve the respective silylamide. In a recent report, Burger and co-workers reported detailed mechanistic studies from a reaction of (PDI)Ir≡N (PDI = 2,6-(ArN=CMe)$_2$C$_5$H$_3$N) with various tertiary silanes, HSiR$_3$.[50]
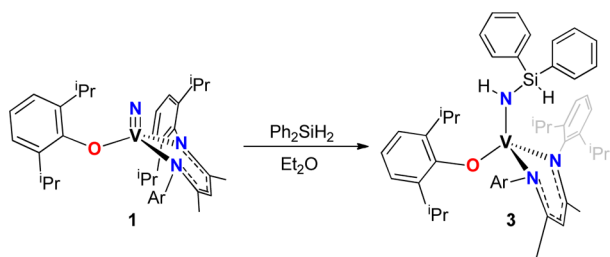
Spectroscopic characterization of **3** by ^{1}H NMR evidenced extremely broad and shifted resonances consistent with a paramagnetic vanadium species. The room-temperature magnetic moment determination by the method of Evans of **3** revealed a μ_{eff} = 2.87 μ_B (C$_6$D$_6$, 298 K) consistent with a high-spin S = 1 V(III) ion. The FT-IR (Nujol) spectrum of **3** also showed sharp and diagnostic stretches at 3338 and 2116 cm^{-1} indicative of N−H and Si−H functional groups, respectively. Solid-state characterization of **3** by XRD confirmed our proposed product, and the molecular structure is shown in Figure 3. The nacnac nitrogen−vanadium distances are conventional at 1.971(4) Å and 1.995(4) Å, as is the vanadium−arylalkoxide bond distance at 1.821(3) Å. The V−N(H)SiHPh$_2$ linkage has a bond distance of 1.916(4) Å, which unequivocally revealed a single bond from the much shorter V≡N of **1**. Lastly, the V(1)−N(3)−Si(1) angle of 122.83° is a convincing indication of a rather planar sp^2 hybridized nitrogen atom (sum of the angles around N3 = 359.95°).

The formation of **3** can possibly proceed by two different pathways: (1) direct nitride insertion into the Si−H bond via a three-center transition state without precoordination of the silane to the vanadium center, or (2) initial formation of nitride−silane adduct followed by [1,2]-migration of the
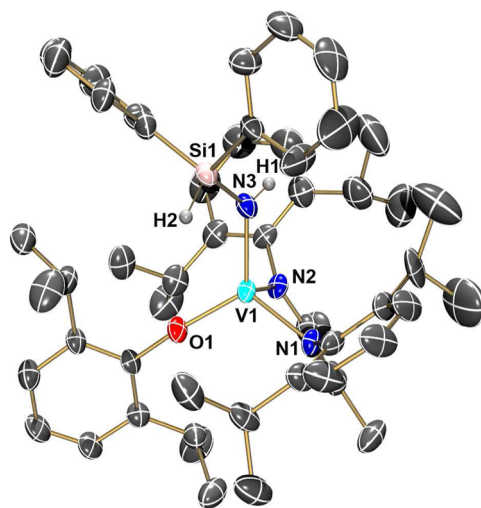
Figure 2. Molecular diagram of (nacnac)V≡N(ODiiP). Only the α orbitals are shown since the β subspace is a mirror image to α subspace for a closed-shell singlet molecule.

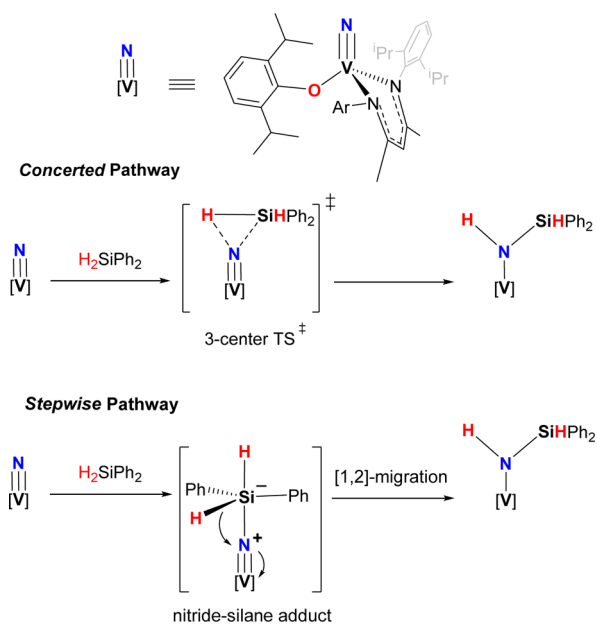**Scheme 5. Addition of a Secondary Silane Si–H Bond to the Nitride Ligand in Complex 1**

hydrogen atom (Scheme 6). As noted before, a reaction pathway featuring a three-center transition state has been proposed for the hydrogenation of a Ir≡N ligand via dihydrogen or silane.[51] The same study investigated the possibility a stepwise mechanism; however, this pathway was ultimately ruled out. Unlike electrophilic nitride systems, in which the LUMO has a large amount of orbital character localized at the terminal nitrogen atom, the LUMO for the vanadium nitride consists of an antibonding combination and is mostly metal-based. Therefore, we hypothesize that the most likely mechanism is initial formation of a nitride–silane adduct given the nucleophilic nature of the vanadium nitride (see DFT vide supra) and energetically accessible σ^*-orbitals at silicon

Figure 3. Molecular structure of **3** with thermal ellipsoids at the 50% probability level. Hydrogen atoms (with the exception of H1 and H2 on amide and silane) were excluded for clarity. Selected bonds distances (Å) and angles (deg): V1–N1 = 1.973(4), V1–N2 = 1.995(4), V1–N3 = 1.914(4), V1–O1 = 1.821(3), N1–V1–N2 = 91.29(18), N1–V1–N3 = 118.22(19), N1–V1–O1 = 112.64(18), N3–V1–O1 = 115.51(18), V1–O1–C(ipso) = 161.1(3).
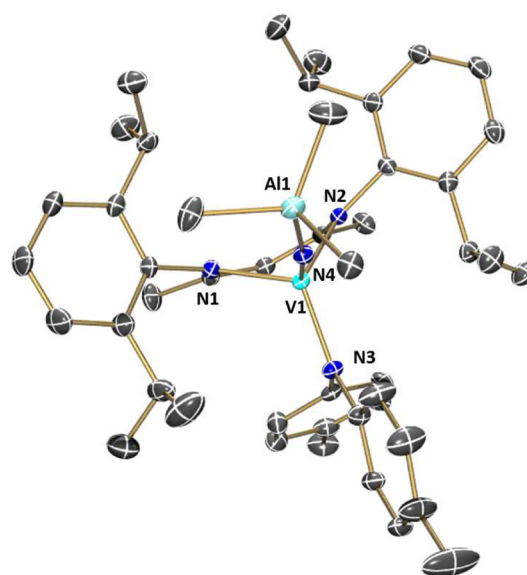
Scheme 6. Two Likely Proposed Reaction Pathways to Formation of 3

Figure 4. Molecular structure of [(nacnac)V{NAlMe₃}(Ntolyl₂)] with thermal ellipsoids at the 50% probability level. Hydrogen atoms were removed for clarity. Selected bonds distances (Å) and angles (deg): V1−N1 = 1.906(18), V1−N2 = 1.9480(17), V1−N3 = 1.9101(18), V1−N4 = 1.6031(17), N4−Al1 = 1.9827(18), Al−Me$_{Ave}$ = 1.985(3), N1−V1−N2 = 97.01(7), V1−N4−Al1 = 169.21(11).

(Scheme 6). A 1,2-H migration would then result in formation of complex **3** in accord with a stepwise mechanism. We were unable to isolate any intermediates prior to formation of the final product, which would help differentiate between the two pathways. A more detailed study addressing these proposed pathways is currently being explored in our laboratories.
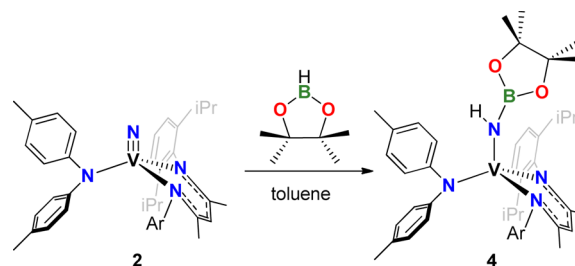
To further support the nucleophilicity of the vanadium nitride and the plausibility of a nitride-silane adduct in route to the formation of **3**, **2** was treated with 1 equiv of AlMe₃. Although a solid-state X-ray structure confirmed formation of the aluminum adduct [(nacnac)V{NAlMe₃}(Ntolyl₂)], this complex was too unstable to characterize unambiguously (see Supporting Information). On the basis of the solid-state structure (Figure 4), the V(1)−N(4) distance has elongated slightly (1.6031(17) Å) relative to related, uncapped nitride species. The aluminum center is now pyramidalized (average N−Al−Me angle = 104.86(9) and the N(4)−Al(1) distance of 1.9827(18)) and in accord with the expected dative bond with no evidence of hyperconjugation into a σ* of the Al−Me bonds. Interestingly, despite the low BDE of the Al−CH₃ bond (BDE = 62.9 kcal/mol) in addition to the strength of the Al−N bond, the nitride does not insert into the Al−CH₃ bond. To our surprise, aluminum-capped nitrides[52] are quite rare especially in which the nitride does not bridge a transition metal.

Treatment of orange **2** with 1 equiv of pinacolborane readily formed the dark green borylamide [(nacnac)V{NH(Bpinacol)-(Ntolyl₂)] (**4**). An IR (Nujol) spectrum of **4** confirms the insertion into a B−H bond with an N−H stretch at 3336 cm⁻¹ (Scheme 7). XRD studies on a single crystal of **4** yield unequivocal evidence for the formation of an N-inserted nitride into a B−H bond (Figure 5). The N4−B1 bond distance of 1.396(5) Å and N4−V1 distance of 1.907(3) Å indicate the stronger Lewis acidity of the boronic ester over the V(III) center as has already been seen in previous 3d systems.[53,54] The π-donation of the nitrogen lone pair to the boron is further supported by the sum of the angles around both N4 and B1, which are 360.00° and 359.97°, respectively. Presumably the
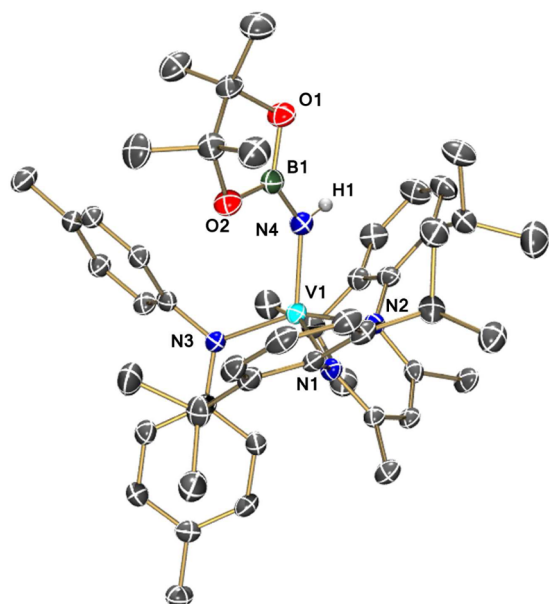
Scheme 7. Addition of a Secondary B−H Bond to the Nitride Ligand in Complex 2

formation of **4** from **2** follows a similar mechanism to that of **1** to **3**, albeit with the nucleophilic nitride coordinating through the accessible p-orbital of the boron.
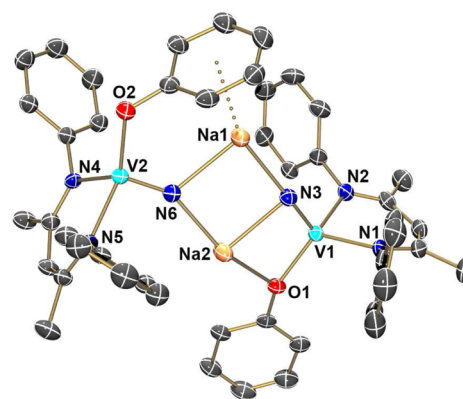
Cyclic Voltammetry and Chemical Reduction of a Vanadium Nitride Complex. Cyclic voltammetry (CV) studies (using 0.3 M tetrabutylammonium hexafluorophosphate (TBAPF₆) in tetrahydrofuran (THF) at 25 °C with ferrocene (Fc)/ferrocenium (Fc⁺) referenced at 0.0 V were performed to understand the redox chemistry of nitridovanadium(V) complexes particularly because vanadium(IV) and vanadium-(III) are common oxidation states. The behavior of the two nitride complexes **1** and **2** are nearly similar and exhibit an irreversible one-electron cathodic wave at −2.0 V assigned to the vanadium(V/IV) couple. At more cathodic potentials, another irreversible wave is observed at −2.8 V, which could quite possibly be the V(IV/III) couple. Analysis of the reduction waves at faster scan rates did not show signs of reversibility in the voltammagram. Surprisingly, scanning anodically reveals a low potential and reversible oxidation wave at −43 and 312 mV for **1** and **2**, respectively. These oxidation waves most likely stem from ligand oxidation and are not metallocentric. Further support for ligand oxidation can be extracted from the electronic structure of **1**, in which the

Figure 5. Molecular structure of **4** with thermal ellipsoids at the 50% probability level. Hydrogen atoms (with the exception of H1 on the amide). Selected bonds distances (Å) and angles (deg): V1−N1 = 1.995(2), V1−N2 = 2.021(3), V1−N3 = 1.966(3), V1−N4 = 1.907(3), N4−B1 = 1.396(5), N1−V1−N2 = 92.41(10), N1−V1−N3 = 114.21(10), N2−V1−N4 = 98.11(11), N3−V1−N2 = 119.05(11), N1−V1−N4 = 116.77(11), N3−V1−N4 = 113.75(11), V1−N4−B1 = 131.3(2).
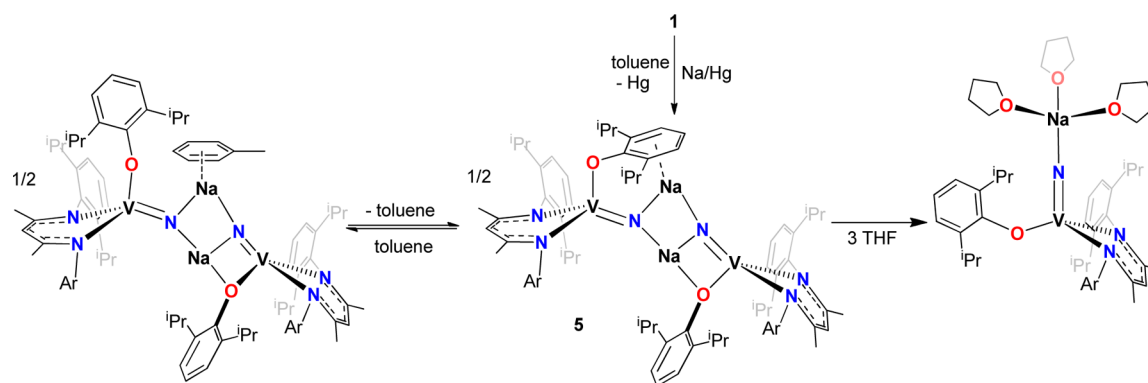

Figure 6. Solid-state structure of **5** shown with thermal ellipsoids at 50% probability level. All hydrogen atoms and isopropyl groups of the nacnac and aryloxide ligands, as well as a pentane molecule, are omitted for clarity. Selected bonds distances (Å) and angles (deg): V1−N1 = 2.051(3), V1−N2 = 2.047(3), V1−N3 = 1.624(3), V1−O1 = 1.920(2), Na1−N3 = 2.336(3), Na1−N6 = 2.405(3), Na1−Ar$_{Centroid}$ = 2.611, Na2−O1 = 2.556(3), V2−O2 = 1.922(2), V2−N6 = 1.614(3), V2−N4 = 2.052(3), V2−N5 = 2.057(3), N4−V2−O2 = 119.51(10), N4−V2−N5 = 88.19(10), O2−V2−N6 = 110.58(12), O2−V2−N5 = 123.91(10), N5−V2−N6 = 105.49(12), N4−V2−N6 = 106.21(12), N6−Na1−N3 = 93.93(10), N6−Na2−N3 = 96.10(10), N3−V1−N2 = 109.13(13), N3−V1−N1 = 106.46(12), N2−V1−N1 = 90.79(11), O1−V1−N1 = 120.12(10), O1−V1−N2 = 119.15(10), O1−V1−N3 = 109.45(12).

conjugated π-system of the aryloxide and anilide ligand dominates the HOMO (Figure 1, vide infra).

Chemical reduction of **1** with 0.5% Na/Hg in toluene at room temperature produced a dark brown crystalline material, which was obtained in pure form in 35% yield from recrystallization from a saturated solution of *n*-pentane at −37 °C. Analysis of a single crystal grown from *n*-pentane by an XRD study provided the connectivity consistent with formation of a radical anionic nitride dimer complex of formula [Na]$_2$[(nacnac)V(N)(OAr)]$_2$ (**5**), depicted in Scheme 8 (synthesis) and Figure 6 (XRD structure). The most salient feature of the solid-state structure is the slight elongation of the vanadium−nitrido bond distance to ~1.62 Å, compared to 1.55 Å for (nacnac)V≡N(ODiiP). Interestingly, the dimeric molecule has two unsymmetrical vanadium(IV) centers with each vanadium conserving an overall distorted tetrahedral geometry (angles are provided in the caption of Figure 6). The
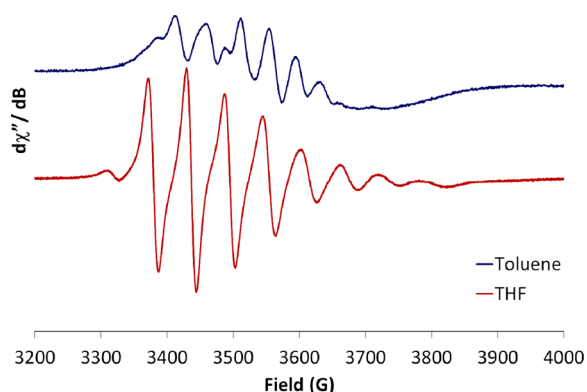
asymmetry stems from each bridging sodium cation exhibiting distinctly different coordination environments. Although both Na$^+$ ions bridge the nitride ligands, one of the aryloxide ligands coordinates via an η^6-aryl hapticity (Na1), while the other interacts with the alkoxide oxygen (Na2). To some degree, the structure observed in **5** resembles other reported group 5 diamagnetic, dimeric anionic nitride complexes of formula [Na][N≡M[N(ᵗBu)Ar]$_3$]$_2$ (M = Nb, V; Ar = 3,5-Me$_2$C$_6$H$_3$) reported by Cummins and co-workers where the aryl motif encapsulates the Na$^+$ ions.[36,37]

On the basis of charge considerations, each vanadium ion in compound **5** is in the +4 oxidation state and should therefore possess one unpaired electron. The room-temperature X-band EPR spectrum of an orange-brown solution of **5** in toluene (Figure 7) exhibited an eight-line pattern as expected for one unpaired electron coupling to I = 7/2 (g_{iso} = 2.01, A_{iso} = 43 G).[6] Despite having two unsymmetrical vanadium centers, we observed only one vanadium(IV) environment suggesting

Scheme 8. Reduction of 1 with Na/Hg to Form the Radical Anion Dimer 5 and Subsequent Solvation with THF

Figure 7. Room-temperature isotropic X-band EPR of **5** recorded in toluene (blue trace) and THF (red trace).

that the solution structure differs from that depicted in the solid state. It is possible that on the EPR time scale at 25 °C, there is fast exchange in which aryloxide ligand is interacting reversibly with the sodium cation and that more than one species is present in solution. Alternatively, toluene might be disrupting the aryloxide π-cation interaction with the sodium ions to generate symmetrically related vanadium centers, but further studies are warranted to understand the fluxional behavior in **5** in solution. We hypothesized that a donor solvent like THF could disrupt the π-cation interaction to favor formation of a discrete monomeric anionic nitride species, whereby the sodium ion has been solvated by THF to form [Na(THF)₃]-[(nacnac)V(N)(OAr)] akin to other monomeric anionic nitridovanadium(V) species (Scheme 8).[39,40] Accordingly, the dissolution of complex **5** in THF produced an olive-green solution that yielded a well-resolved isotropic EPR spectrum (Figure 7) with the eight-line pattern consistent of a V(IV) ion (g_{iso} = 1.97, A_{iso} = 58 G).[6] Unfortunately, all efforts thus far to simulate well either EPR spectrum have failed. Complex **5** represents a nitridyl analogue for the ubiquitous vanadyl ion. Although nitridyl salts of vanadium are unknown, a number of isovalent d¹ Cr(V) species have been reported in the literature;[55−57] however, these typically exist in a tetragonal geometry.

CONCLUSIONS

The preconception that early metal nitrides are unreactive spectator ligands is false. Our investigation clearly shows that early 3d metal nitrides can undergo further reactivity at the nitride functionality in conjunction with redox shuffling at vanadium. The low-coordinate vanadium center coupled to the multitude of oxidation states that this metal ion can access has allowed us to add Si−H and B−H bonds to afford a coordinated silyl or borylamido ligands. The nucleophilicity of the nitride moiety was further confirmed by observation of an aluminum-capped species, also supporting (albeit indirectly) our proposed stepwise mechanism for E−H bond addition. A radical anion of a vanadium nitride has been also prepared by one-electron reduction of the neutral vanadium(V) nitride. We are presently determining if these nitride radical anions show any chemistry reminiscent of late-transition metal nitridyls.[47,49,58]

EXPERIMENTAL SECTION

General Considerations. Unless otherwise stated, all operations were performed in an M. Braun Lab Master double-drybox under an atmosphere of purified nitrogen or using high-vacuum standard Schlenk techniques under a nitrogen atmosphere. Anhydrous *n*-hexanes, *n*-pentane, toluene, and benzene were purchased from Aldrich in sure-sealed reservoirs (18 L) and dried by passage through two columns of activated alumina and a Q-5 column. Diethyl ether and CH₂Cl₂ were dried by passage through a column of activated alumina. THF was distilled, under nitrogen, from purple sodium benzophenone ketyl and stored under sodium metal. Distilled THF was transferred under vacuum into bombs before being pumped into a drybox. C₆D₆ was purchased from Cambridge Isotope Laboratory, degassed, and vacuum-transferred to 4 Å molecular sieves. Celite, alumina, and 4 Å molecular sieves were activated under vacuum overnight at 200 °C. Compounds **1** and **2** were prepared according to literature procedures.[30,59] All other chemicals were used as received from Sigma-Aldrich unless otherwise stated. ¹H, ¹³C, ⁵¹V, and ¹⁵N NMR spectra were recorded on Varian 300, 400, and 500 MHz NMR spectrometer. ¹H and ¹³C NMR spectra are reported with reference to solvent resonances of C₆D₆ at 7.16 and 128.0 ppm, respectively. X-ray diffraction data were collected on a SMART6000 (Bruker) system under a stream of N₂ (g) at low temperatures. Elemental analysis was performed at Indiana University, Bloomington. Infrared spectroscopy was performed on the Thermo Nicolet 6700 FT-IR equipped with software under PC control.

Synthesis of [(nacnac)V{N(H)SiHPh₂}(OAr)] (3). In a 20 mL scintillation vial was charged **2** (75 mg, 0.11 mmol), a magnetic stir bar, and 10 mL of Et₂O. To the yellow solution was added H₂SiPh₂ (50.0 mg, 0.27 mmol) leading to a gradual color change to dark green. The reaction mixture was stirred for an additional 10 h. Subsequent filtration through medium porosity frit containing Celite and reduction to 3 mL in volume and storage at −37 °C overnight produced crystalline product. The crystalline product was collected via vacuum filtration with a medium porosity frit and dried under reduced pressure. Yield = 61% (139 mg, 0.16 mmol). ¹H NMR (25 °C, 400 MHz, C₆D₆): δ 10.73 ($\Delta\nu_{1/2}$ = 154 Hz), 9.63 ($\Delta\nu_{1/2}$ = 225 Hz), 8.59 ($\Delta\nu_{1/2}$ = 803 Hz), 7.35 ($\Delta\nu_{1/2}$ = 24 Hz), 6.99 ($\Delta\nu_{1/2}$ = 43 Hz), 4.73 ($\Delta\nu_{1/2}$ = 205 Hz), 3.56 ($\Delta\nu_{1/2}$ = 13 Hz) 3.38 ($\Delta\nu_{1/2}$ = 88 Hz), 2.52 ($\Delta\nu_{1/2}$ = 206 Hz), 1.41 ($\Delta\nu_{1/2}$ = 168 Hz), −4.09 ($\Delta\nu_{1/2}$ = 117 Hz). FT-IR (KBr, Nujol, cm⁻¹): 3338 (N−H), 2116 (Si−H). μ_{eff} = 2.87 μ_B (Evans, 25 °C). Anal. Calcd for C₅₃H₇₀N₃OSiV: C, 75.41; H, 8.36; N, 4.98. Found: 75.35; H, 8.11; N, 5.02%.

Synthesis of [(nacnac)V{NAlMe₃}(Ntolyl₂)].)Complex **2** (36 mg, 0.05 mmol) was dissolved into 2 mL of C₆D₆ and transferred to a J. Young NMR tube. To the orange solution was added a hexane solution of AlMe₃ via a microliter syringe (30 μL, 0.06 mmol) leading to a slight color change to darker red-orange. After 30 min the solvent was removed under reduced pressure and extracted into minimal pentane and transferred to a 20 mL scintillation vial. Storage at −37 °C overnight produced crystalline product. The crystalline product was collected via vacuum filtration with a medium porosity frit and dried under reduced pressure. Yield = 40.0% (15 mg, 0.04 mmol). This compound decomposed in solution so characterization of this species in pure form was not possible.

Synthesis of [(nacnac)V{N(H)Bpinacol}(Ntolyl₂)] (4). In a 20 mL scintillation vial was charged **1** (75 mg, 0.11 mmol), a magnetic stir bar, and 10 mL of toluene. To the stirring solution was added pinacolborane (14 mg, 0.11 mmol) dropwise. The orange solution instantly changed to dark green. The reaction proceeded for an additional 10 min to ensure full consumption of the starting materials at which point the solution was filtered through a 2 in. plug of Celite. The plug was washed with 5 mL of pentane to remove any residual material from the Celite. The solvent was removed under reduced pressure to give a dark brown-green oil, which was extracted into 3 mL of pentane. X-ray quality single crystals were grown by a slow evaporation of the pentane solution at −37 °C. Yield = 46% (41 mg, 0.05 mmol). ¹H NMR (25 °C, 400 MHz, C₆D₆): δ 10.22 ($\Delta\nu_{1/2}$ = 202 Hz), 7.72 ($\Delta\nu_{1/2}$ = 95 Hz), 5.07 ($\Delta\nu_{1/2}$ = 161 Hz), 3.26 ($\Delta\nu_{1/2}$ = 121 Hz), 1.04 ($\Delta\nu_{1/2}$ = 9.92 Hz), −1.17 ($\Delta\nu_{1/2}$ = 107.14 Hz). FT-IR (KBR, NuJol, cm⁻¹) 3336 (N−H). μ_{eff} = 2.36 μ_B (Evans, 25 °C). Note: **4** appears to be thermally unstable as C₆D₆ solutions seem to decompose to an unidentified, brown paramagnetic product over the

period of hours at room temperature. Because of the thermal instability of **4** we were unable to get reliable combustion analysis.

Synthesis of [Na]$_2$[(nacnac)V(N)(OAr)]$_2$ (5). In a 20 mL scintillation vial was charged **1** (216 mg, 0.32 mmol), a magnetic stir bar, and 10 mL of toluene. To the vigorously stirring mixture was added 0.5% Na/Hg (10 mg Na, 1.80 g Hg). The yellow solution gradually turned brown. After it was stirred for 4 h, the reaction mixture was filtered through a medium-porosity frit containing Celite to remove salt residues and sodium amalgam. Subsequently, all volatiles were removed under reduced pressure. The crude product was extracted into 5 mL of *n*-pentane and filtered and stored at −37 °C to afford dark brown crystalline product, which was collected and dried under reduced pressure. Yield = 35%. μ_{eff} = 1.89 μ_{B} (Evans, 25 °C). X-band EPR (25 °C): g_{iso} = 2.01, A_{iso} = 43 G (toluene); g_{iso} = 1.97, A_{iso} = 58 G (THF). Anal. Calcd for C$_{82}$H$_{116}$N$_6$Na$_2$V$_2$: C, 72.12; H, 8.56; N, 6.15. Found: C, 72.40; H, 8.45; N, 6.39%.

Crystallographic Studies for Compounds 3 and 5. Inert-atmosphere techniques were used to place the crystal onto the tip of a glass capillary mounted on a SMART6000 (Bruker) at 150 K. A preliminary set of cell constants was calculated from reflections obtained from three nearly orthogonal sets of frames. The data collection was carried out using graphite monochromated Mo Kα (λ = 0.710 73 Å) radiation with appropriate time frame. A randomly oriented region of a sphere in reciprocal space was surveyed. In general, three sections of frames were collected with 0.30° steps in ω at different φ settings with the detector set at −43° in 2θ. Final cell constants were calculated from the *xyz* centroids of strong reflections from the actual data collection after integration (SAINT[60]). The structure was solved using SHELXS-97 and refined with SHELXL-97.[61]

Crystallographic Studies for Compound [(nacnac)V-{NAlMe$_3$}(Ntolyl)]. An orange crystal was placed onto the tip of an ultrathin glass rod and mounted on a D8 platform goniometer and measured at 100(2) K. The data collection was carried out using synchrotron radiation (λ = 41 328 Å, *E* = 30 keV, silicon 1 1 1 and 3 1 1 monochromators, and two mirrors to exclude higher harmonics) with a frame time of 0.3 s and a detector distance of 8.0 cm. A randomly oriented region of reciprocal space was surveyed to the extent of a hemisphere. The total exposure time was 0.12 h. The frames were integrated with the Bruker SAINT software package[60] using a narrow-frame algorithm. The integration of the data using a monoclinic unit cell yielded a total of 31 832 reflections to a maximum θ angle of 28.31° (0.75 Å resolution), of which 10 546 were independent (average redundancy 3.018, completeness = 96.8%, R_{int} = 4.67%, R_{sig} = 5.48%) and 8177 (77.54%) were greater than 2σ(F^2). Data were corrected for absorption effects using the multiscan method (SADABS).

Crystallographic Studies for Compound 4. Inert-atmosphere techniques were used to place the crystal onto the tip of a glass capillary, and X-ray intensity data were collected on a Bruker APEXII CCD area detector employing graphite-monochromated Mo Kα radiation (*l* = 0.71073 Å) at a temperature of 100(1) K. Preliminary indexing was performed from a series of 36 rotation frames (0.5°) with exposures of 10 s. A total of 1913 frames were collected with a crystal-to-detector distance of 37.4 mm, rotation widths of 0.5°, and exposures of 40 s. It was obvious from the beginning of data collection that the sample was a "multiple-crystal" (many random, double- and triple-spots on the diffraction frames). Three components were identified by CELL_NOW,[62] and the sample was treated as a nonmerohedral twin. Rotation frames were integrated using SAINT,[60] producing a listing of unaveraged F^2 and $s(F^2)$ values, which were then passed to the SHELXTL[61] program package for further processing and structure solution. A total of 110 629 reflections were measured over the ranges of 1.78 ≤ θ ≤ 27.54°, −14 ≤ *h* ≤ 15, −15 ≤ *k* ≤ 15, and 0 ≤ *l* ≤ 22 yielding 10 227 unique reflections (R_{int} = 0.1009). The intensity data were corrected for Lorentz and polarization effects and for absorption using TWINABS[63] (minimum and maximum transmission 0.4786, 0.7456). The structure was solved by direct methods (SHELXS-97). Refinement was by full-matrix least-squares fit based on F^2 using SHELXL-97. All reflections were used during refinement.

Measurement Conditions for Cyclic Voltammetry Studies. The CV measurements were performed in predried and recrystallized 0.3 M TBAPF$_6$ in anhydrous THF solution. A platinum disk (2.0 mm diameter), a platinum wire, and silver wire were employed as the working electrode, the auxiliary, and the reference electrode, respectively. A one compartment cell was used in the CV measurement. The electrochemical response was collected with the assistance of an E2 Epsilon (BAS) autolab potentiostat/galvanostat under control by BAS software. All of the potentials were reported against the Fc$^+$/Fc couple (0.0 V). The IR drop correction was applied when significant resistance was noted. All the potentials were reported. The spectrum was recorded under a N$_2$ atmosphere in the glovebox. In a typical experiment 15 mg of metal complex was dissolved in 5 mL of a TBAPF$_6$ solution in THF at 25 °C.

Computational Studies. All calculations were performed using DFT as implemented in the Jaguar 7.0 suite of ab initio quantum chemistry programs. Geometry optimizations were performed with the B3LYP[64−67] and the 6-31G** basis set with no symmetry restrictions. Transition metals were represented using the Los Alamos LACVP basis.[68−70] The models used in this study consist of up to ∼100 atoms, which represent the nontruncated molecules that were also used in the related experimental work.

■ ASSOCIATED CONTENT

Ⓢ Supporting Information

Crystallographic tables, illustrated molecular structures, cyclic voltammogram of **1**, 1H NMR and FT-IR spectral data, molecular modeling coordinates, modeling programs, and complete crystallographic information files (CIF). This material is available free of charge via the Internet at http://pubs.acs.org.

■ AUTHOR INFORMATION

Corresponding Author
*E-mail: mindiola@sas.upenn.edu.

Present Address
‡University of Pennsylvania, Department of Chemistry, 231 South 34th Street, Philadelphia, Pennsylvania 19104.

Notes
The authors declare no competing financial interest.

■ ACKNOWLEDGMENTS

■ REFERENCES

(1) Eikey, R. A.; Abu-Omar, M. M. *Coord. Chem. Rev.* **2003**, *243*, 83.

(2) Berry, J. F. *Comments Inorg. Chem.* **2009**, *30*, 28.

(3) Williams, D. S.; Meyer, T. J.; White, P. S. *J. Am. Chem. Soc.* **1995**, *117*, 823.

(4) McCarthy, M. R.; Crevier, T. J.; Bennett, B.; Dehestani, A.; Mayer, J. M. *J. Am. Chem. Soc.* **2000**, *122*, 12391.

(5) Crevier, T. J.; Bennett, B. K.; Soper, J. D.; Bowman, J. A.; Dehestani, A.; Hrovat, D. A.; Lovell, S.; Kaminsky, W.; Mayer, J. M. *J. Am. Chem. Soc.* **2001**, *123*, 1059.

(6) Schoffel, J.; Rogachev, A. Y.; George, S. D.; Burger, P. *Angew. Chem., Int. Ed.* **2009**, *48*, 4734.

(7) Yi, X.-Y.; Lam, T. C. H.; Sau, Y.-K.; Zhang, Q.-F.; Williams, I. D.; Leung, W.-H. *Inorg. Chem.* **2007**, *46*, 7193.

(8) Scepaniak, J. J.; Young, J. A.; Bontchev, R. P.; Smith, J. M. *Angew. Chem., Int. Ed.* **2009**, *48*, 3158.

(9) Thomson, R. K.; Cantat, T.; Scott, B. L.; Morris, D. E.; Batista, E. R.; Kiplinger, J. L. *Nat. Chem.* **2010**, *2*, 723.

(10) Schoffel, J.; Susnjar, N.; Nuckel, S.; Sieh, D.; Burger, P. *Eur. J. Inorg. Chem.* **2010**, 4911.

(11) Long, A. K.; Timmer, G. H.; Pap, J. S.; Snyder, J. L.; Yu, R. P.; Berry, J. F. *J. Am. Chem. Soc.* **2011**, *133*, 13138.

(12) Crevier, T. J.; Mayer, J. M. *Angew. Chem., Int. Ed.* **1998**, *37*, 1891.

(13) Brown, S. N. *J. Am. Chem. Soc.* **1999**, *121*, 9752.

(14) Ware, D. C.; Taube, H. *Inorg. Chem.* **1990**, *30*, 4605.

(15) Betley, T. A.; Peters, J. C. *J. Am. Chem. Soc.* **2004**, *126*, 6252.

(16) Man, W.-L.; Tang, T.-M.; Wong, T.-W.; Lau, T.-C.; Peng, S.-M.; Wong, W.-T. *J. Am. Chem. Soc.* **2004**, *126*, 478.

(17) Laplaza, C. E.; Cummins, C. C. *Science* **1995**, *268*, 861.

(18) Laplaza, C. E.; Johnson, M. J. A.; Peters, J. C.; Odom, A. L.; Kim, E.; Cummins, C. C.; George, G. N.; Pickering, I. J. *J. Am. Chem. Soc.* **1996**, *118*, 8623.

(19) Curley, J. J.; Cook, T. R.; Reece, S. Y.; Muller, P.; Cummins, C. C. *J. Am. Chem. Soc.* **2008**, *130*, 9394.

(20) Schrock, R. R.; Listemann, M. L.; Sturgeoff, L. G. *J. Am. Chem. Soc.* **1982**, *104*, 4291.

(21) Gdula, R. L.; Johnson, M. J. A. *J. Am. Chem. Soc.* **2006**, *128*, 9614.

(22) Heppekausen, J.; Stade, R.; Goddard, R.; Furstner, A. *J. Am. Chem. Soc.* **2010**, *132*, 11045.

(23) Fürstner, A. *Angew. Chem., Int. Ed.* **2013**, *52*, 2794.

(24) Finke, A. D.; Moore, J. S. *Chem. Commun.* **2010**, *46*, 7939.

(25) Neyman, K. M.; Nasluzov, V. A.; Hahn, J.; Landis, C. R.; Rösch, N. *Organometallics* **1997**, *16*, 995.

(26) Cui, Q.; Musaev, D. G.; Svensson, M.; Sieber, S.; Morokuma, K. *J. Am. Chem. Soc.* **1995**, *117*, 12366.

(27) Sceats, E. L.; Figueroa, J. S.; Cummins, C. C.; Loening, N. M.; Van der Wel, P.; Griffin, R. G. *Polyhedron* **2004**, *23*, 2751.

(28) Curley, J. J.; Cozzolino, A. F.; Cummins, C. C. *Dalton Trans.* **2011**, *40*, 2429.

(29) Silvia, J. S.; Cummins, C. C. *J. Am. Chem. Soc.* **2008**, *131*, 446.

(30) Tran, B. L.; Pink, M.; Gao, X.; Park, H.; Mindiola, D. J. *J. Am. Chem. Soc.* **2010**, *132*, 1458.

(31) Tran, B. L.; Thompson, R.; Ghosh, S.; Gao, X.; Chen, C.-H.; Baik, M.-H.; Mindiola, D. J. *Chem. Commun.* **2013**, *49*, 2768.

(32) Tran, B. L.; Pink, M.; Gao, X.; Park, H.; Mindiola, D. J. *J. Am. Chem. Soc.* **2010**, *132*, 1458.

(33) Tran, B. L.; Krzystek, J.; Ozarowski, A.; Chen, C.-H.; Pink, M.; Karty, J. A.; Telser, J.; Meyer, K.; Mindiola, D. J. *Eur. J. Inorg. Chem.* **2013**, *2013*, 3916.

(34) Willing, W.; Christophersen, R.; Muller, U.; Dehnicke, K. *Z. Anorg. Allg. Chem.* **1987**, *555*, 16.

(35) Critchlow, S. C.; Lerchen, M. E.; Smith, R. C.; Doherty, N. M. *J. Am. Chem. Soc.* **1988**, *110*, 8071.

(36) Brask, J. K.; Dura-Vila, V.; Diaconescu, P. L.; Cummins, C. C. *Chem. Commun.* **2002**, 902.

(37) Brask, J. K.; Fickes, M. G.; Sangtrirutnugul, P.; Dura-Vila, V.; Odom, A. L.; Cummins, C. C. *Chem. Commun.* **2001**, 1676.

(38) Song, J.-I.; Gambarotta, S. *Chem.—Eur. J.* **1996**, *2*, 1258.

(39) Henderson, R. A.; Janas, Z.; Jerzykiewicz, L. B.; Richards, R. L.; Sobota, P. *Inorg. Chim. Acta* **1999**, *285*, 178.

(40) Song, J.-I.; Gambarotta, S. *Chem.—Eur. J.* **1996**, *2*, 1258.

(41) Chiu, H.-T.; Chen, Y.-P.; Chuang, S.-H.; Jen, J.-S.; Lee, G.-H.; Peng, S.-M. *Chem. Commun.* **1996**, 139.

(42) Tran, B. L.; Singhal, M.; Park, H.; Lam, O. P.; Pink, M.; Krzystek, J.; Ozarowski, A.; Telser, J.; Meyer, K.; Mindiola, D. J. *Angew. Chem., Int. Ed.* **2010**, *49*, 9871.

(43) Crevier, T. J.; Bennett, B. K.; Soper, J. D.; Bowman, J. A.; Dehestani, A.; Hrovat, D. A.; Lovell, S.; Kaminsky, W.; Mayer, J. M. *J. Am. Chem. Soc.* **2001**, *123*, 1059.

(44) Sieh, D.; Burger, P. *Z. Anorg. Allg. Chem.* **2014**, DOI: 10.1002/zaac.201400235.

(45) Long, A. K. M.; Yu, R. P.; Timmer, G. H.; Berry, J. F. *J. Am. Chem. Soc.* **2010**, *132*, 12228.

(46) Atienza, C. C. H.; Bowman, A. C.; Lobkovsky, E.; Chirik, P. J. *J. Am. Chem. Soc.* **2010**, *132*, 16343.

(47) Scheibel, M. G.; Askevold, B.; Heinemann, F. W.; Reijerse, E. J.; de Bruin, B.; Schneider, S. *Nat. Chem.* **2012**, *4*, 552.

(48) Scheibel, M. G.; Wu, Y.; Stückl, A. C.; Krause, L.; Carl, E.; Stalke, D.; de Bruin, B.; Schneider, S. *J. Am. Chem. Soc.* **2013**, *135*, 17719.

(49) Gloaguen, Y.; Rebreyend, C.; Lutz, M.; Kumar, P.; Huber, M.; van der Vlugt, J. I.; Schneider, S.; de Bruin, B. *Angew. Chem., Int. Ed.* **2014**, *53*, 6814.

(50) Sieh, D.; Schoffel, J.; Burger, P. *Dalton Trans.* **2011**, *40*, 9512.

(51) Sieh, D.; Burger, P. *J. Am. Chem. Soc.* **2013**, *135*, 3971.

(52) MacKay, B. A.; Patrick, B. O.; Fryzuk, M. D. *Organometallics* **2005**, *24*, 3836.

(53) Warren, T. H.; Schrock, R. R.; Davis, W. M. *Organometallics* **1996**, *15*, 562.

(54) Chen, H.; Bartlett, R. A.; Olmstead, M. M.; Power, P. P.; Shoner, S. C. *J. Am. Chem. Soc.* **1990**, *112*, 1048.

(55) Groves, J. T.; Takahashi, T.; Butler, W. M. *Inorg. Chem.* **1983**, *22*, 884.

(56) Azuma, N.; Imori, Y.; Yoshida, H.; Tajima, K.; Li, Y.; Yamauchi, J. *Inorg. Chim. Acta* **1997**, *266*, 29.

(57) Meyer, K.; Bendix, J.; Bill, E.; Weyhermüller, T.; Wieghardt, K. *Inorg. Chem.* **1998**, *37*, 5180.

(58) Tran, B. L.; Washington, M. P.; Henckel, D. A.; Gao, X.; Park, H.; Pink, M.; Mindiola, D. J. *Chem. Commun.* **2012**, *48*, 1529.

(59) Tran, B. L.; Pinter, B.; Nichols, A. J.; Konopka, F. T.; Thompson, R.; Chen, C.-H.; Krzystek, J.; Ozarowski, A.; Telser, J.; Baik, M.-H.; Meyer, K.; Mindiola, D. J. *J. Am. Chem. Soc.* **2012**, *134*, 13035.

(60) Bruker. *SAINT*; Bruker AXS Inc.: Madison, WI, 2009.

(61) Bruker. *SHELXTL*; Bruker AXS Inc.: Madison, WI, 2009.

(62) Sheldrick, G. M. *CELL_NOW*; University of Gottingen: Germany, 2008.

(63) Sheldrick, G. M. *TWINABS*; University of Gottingen: Germany, 2008.

(64) Becke, A. D. *Phys. Rev. A* **1988**, *38*, 309858.

(65) Becke, A. D. *J. Chem. Phys.* **1993**, *98*, 5648.

(66) Vosko, S. H.; Wilk, L.; Nusair, M. *Can. J. Phys.* **1980**, *58*, 1200.

(67) Lee, C. T.; Yang, W. T.; Parr, R. G. *Phys. Rev. B* **1988**, *37*, 785.

(68) Hay, P. J.; Wadt, W. R. *J. Chem. Phys.* **1985**, *82*, 270.

(69) Hay, P. J.; Wadt, W. R. *J. Chem. Phys.* **1985**, *82*, 299.

(70) Wadt, W. R.; Hay, P. J. *J. Chem. Phys.* **1985**, *82*, 284.